JOURNAL OF PROPULSION AND POWER
Vol. 15, No. 2, March–April 1999

Numerical Analysis of Wells Turbine Aerodynamics

J. K. Watterson* and S. Raghunathan†
Queen's University of Belfast, Belfast, Northern Ireland BT9 5AG, United Kingdom

Ocean wave power can be harnessed by means of a Wells turbine driven by a bi-directional airflow above an oscillating water column. While the Wells turbine research budget remains small, full-scale experiments are prohibitively expensive. Computational fluid dynamics (CFD) is a possible way of generating full-scale data. This paper summarizes a numerical study of Wells turbine performance and aerodynamics using a CFD method, and makes recommendations about its use for Wells turbine studies. Calculations have been performed for a monoplane turbine comprised of straight NACA 0015 blades at a stagger angle of 90 deg, Reynolds number 8×10^5, tip Mach number 0.4, and hub-to-tip ratio 0.6. Flow coefficient, tip clearance, and blade number were varied. The predictions agree favorably with experimental data. Differences can be explained partly by geometric differences between the experimental and numerical turbines. Because of the 90-deg stagger angle of the turbine, accurate predictions require fine resolution of the blade leading-edge region. This makes performance calculations expensive, and it is probably more prudent to use simpler predictive methods. CFD, however, is most useful for the study of turbine aerodynamics.

Nomenclature

C_T = torque coefficient
c = blade chord
h = ratio of hub diameter to tip diameters
N = number of blades in annulus
p_1, p_2 = static pressure up- and downstream of turbine
$\dot{Q}$ = volume flow rate
Q_R = volume flow rate ratio
R_t = tip radius of turbine
T = torque
U_t = blade tip velocity
V_x = axial velocity
Δp^* = nondimensionalized pressure drop
η = efficiency
θ = tangential coordinate
σ = turbine solidity, $Nc/[\pi R_t(1 + h)]$
τ_c = blade clearance at tip as percentage of chord
ϕ = flow coefficient
Ω = angular velocity of turbine

Introduction

UNEVEN solar heating of the Earth's surface, the cycle of day and night, the Earth's rotation, and the gravitational pull of the moon combine to create the awesome store of mechanical energy in the oceans of the world that we experience as currents, tides, and waves. This energy resource is an alternative to fossil fuels, which, when harnessed both economically and with minimum environmental impact, will be particularly attractive to coastal communities. The western coastlines of the United Kingdom and Ireland, which are exposed to the North Atlantic Ocean, are particularly well placed to harvest this energy resource, and it is estimated that the annual average wave power in this region is of the order of 120 GW.[1] Conscious of this fact, about two decades ago, the government of the United Kingdom took an active interest in wave power, setting up nationally coordinated research activities at several establishments, one of which was at the Queen's University of Belfast (QUB). Of the several devices investigated, one of the most successful methods for wave power conversion was that based on the principle of an oscillating water column (OWC) harnessed to a Wells turbine. This device consists of a collecting chamber in which the water level is allowed to rise and fall in sympathy with the waves. One or more ducts, housing the turbines, are connected to the chamber, and a bidirectional flow of air is driven in these ducts by the hydraulic energy in the OWC. The pneumatic energy in the airflow is converted into mechanical energy by means of Wells turbines (Fig. 1), which in their simplest form, comprise a number of symmetrical aerofoil blades positioned around a hub with their chord planes normal to the axis of rotation. The turbine is designed so that it rotates in the same direction, irrespective of the direction of the airflow, such that rectifying valves are unnecessary. Finally, the turbine drives an electrical generator. The QUB research team designed and constructed an OWC/Wells turbine device on the island of Islay, off western Scotland,[2] and this has provided a rich source of multidisciplinary research.

The use of computational fluid dynamics (CFD) to study Wells turbine aerodynamics is relatively novel, despite the wide use of CFD for the study of turbomachinery aerodynamics. Wells turbine research is run on a relatively small budget, and full-scale experimental tests are generally not possible. It is of interest, therefore, to determine the validity of CFD as a complementary research tool that can be used at full-scale Reynolds numbers. A study of the use of a particular CFD code to investigate the performance of a Wells turbine has been performed, and the results are summarized in this paper. The CFD method uses unstructured meshes, which will eventually allow inclusion of features such as blade tip and casing treatments. Here, however, a typical monoplane turbine is modeled, allowing an investigation of the competence of the numerical method. The paper concludes the work previously reported in Refs. 3 and 4, and makes suggestions about the use of CFD for Wells turbine development.

Numerical Method

The numerical method used in this study is the unstructured mesh method of Dawes,[5] called NEWT. The code was origi-

Received Nov. 22, 1997; presented as Paper 98-0363 at the AIAA 36th Aerospace Sciences Meeting, Reno, NV, Jan. 12–15, 1998; revision received Nov. 10, 1998; accepted for publication Nov. 10, 1998.

*Lecturer, School of Aeronautical Engineering, Stranmillis Road. E-mail: j.watterson@queens-belfast.ac.uk.

†Professor, Head of School of Aeronautical Engineering, Stranmillis Road. Senior Member AIAA.

Table 1 Modeled and experimental turbines

	Calculation	Experimental
Aerofoil section	NACA 0015	NACA 0012
Number of blades (solidity)	4 (0.32), 6 (0.48), 8 (0.64)	4 (0.29), 6 (0.44), 8 (0.59)
Tip diameter	0.5 m	0.6 m
Hub-to-tip ratio	0.6	0.5
Tip clearance	0, 1, 2, 4, 6%	1%
Angular speed	5000 rpm	2700 rpm
Tip Mach number	0.40	0.25
Reynolds number	8.0×10^5	5.6×10^5

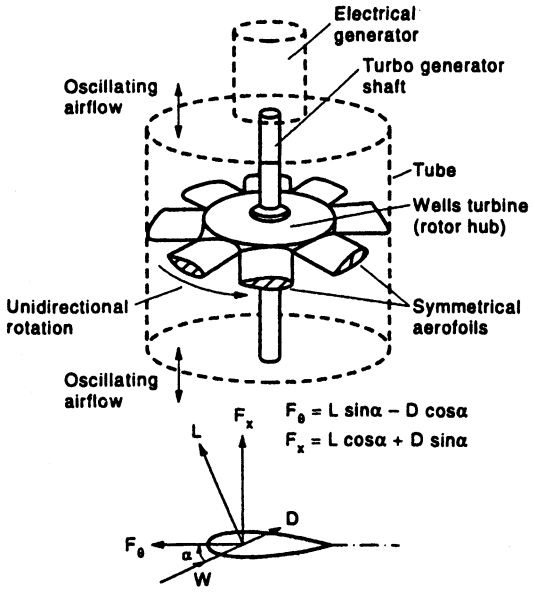

Fig. 1 Schematic of the Wells turbine.

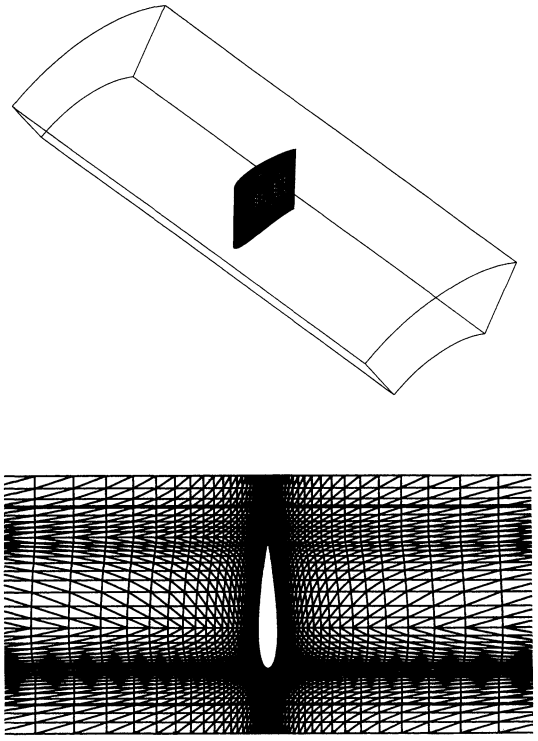

Fig. 2 Computational domain showing perspective view of mesh on turbine blade and mesh on plane of constant radius.

nally developed for turbomachinery applications and has undergone an extensive period of validation for two- and three-dimensional cascades, and axial and radial machines, generally with regions of separated flow. It has been successfully used in the study of a large number of turbomachinery flows[5–7] as well as several nonturbomachinery applications.[8,9]

The method solves discretizations of the fully three-dimensional, unsteady, Reynolds-averaged Navier–Stokes equations, expressed in strong conservation form. Turbulence closure is provided by the k-ε model, together with standard wall functions. For very fine meshes, a modification of the low-Reynolds number model of Lam and Bremhorst[10] is used to handle the near-wall regions. The seven equations of motion are cast in the absolute frame and are solved using the finite volume method of Jameson and Baker,[11] in which the net flux imbalance into each cell is used to update the flowfield variables at the nodes, using four-stage Runge–Kutta time integration. The method is formally time accurate, but maximum local time steps were used in this work to enhance convergence because steady-state solutions were sought. Mass conservation and rms axial residuals are monitored to determine convergence.

Calculations

Computational Domain

The geometry chosen for these calculations is summarized in Table 1. The blade is of constant, untwisted section, and was set with its midchordline aligned with a radius from the axis of rotation, giving the leading-edge effective backsweep. Solidity was varied by changing the width of the computational domain. This is equivalent to changing the blade number N. For the six-blade geometry, the tip clearance was varied so that the effect of this could be studied. The computational domain was extended 3.2 chord lengths upstream and downstream of the blade annulus, and was restricted to one blade-to-blade passage, with periodic boundaries. The computational domain for the case $N = 6$ is shown in Fig. 2.

Mesh

The meshes were created from structured meshes of hexahedra, and different mesh distributions were used for the studies of the effects of tip clearance ratio and solidity. For the tip clearance study, the radial mesh distribution was concentrated around the tip region so that the variation in clearance gap could be obtained easily; as a consequence, mesh was sparse in the hub region. A typical mesh contained about 85,000 nodes. In contrast, the study of solidity required extra mesh in the tangential direction to provide reasonable mesh support in the blade leading-edge region for the lowest solidity case. This resulted in meshes of about 140,000 nodes. Typically, y^+ for the first node adjacent to the blade suction surface was 25 at midchord and midspan.

Boundary Conditions

At the inflow boundary, the total temperature and velocity are specified. Static pressure is extrapolated, and density and total internal energy are calculated. Inflow values of turbulent kinetic energy k and dissipation rate ε are also specified; in particular, the turbulence level is 1% of the reference flow speed. Setting the inflow velocity allows the flow coefficient

to be specified. Flow coefficient is defined as the ratio of the average inlet axial velocity to the tangential blade tip speed:

$$\phi = V_x/U_t \tag{1}$$

The values of flow coefficient used were 0.08, 0.10, 0.12, and 0.15.

At the outflow boundary, static pressure is specified. For these calculations, an estimate of the exit swirl was made so that a radial static pressure distribution could be set. Density, velocity, and the turbulence quantities are extrapolated and total internal energy is calculated. The hub, casing, and blade tip are treated as inviscid surfaces, and only the blade surface is treated as viscous. Wall functions are used to estimate the skin friction and the wall values of k and ε wherever the y^+ value of the node adjacent to the viscous wall is greater than 10.

Discussion

Turbine Performance

First, it will be shown that the numerical method is able to predict the performance of the turbine with reasonable accuracy. Experimental data are available from Gato and Falcao[12] for a very similar set of turbines, and this will be used for comparison with the predictions. Table 1 includes a summary of the geometries used in the experimental study.

Three performance parameters will be used in the comparison: pressure drop Δp^*, torque coefficient C_T, and efficiency η. Pressure drop is defined as the change in mean static pressure across the computational domain $(p_1 - p_2)$, nondimensionalized with respect to twice the tip relative dynamic head:

$$\Delta p^* = (p_1 - p_2)/\rho\Omega^2 R_t^2 \tag{2}$$

where R_t is the tip radius. The torque coefficient is obtained by nondimensionalizing the turbine torque with respect to $\rho\Omega^2 R_t^2$, i.e.,

$$C_T = T/\rho\Omega^2 R_t^5 \tag{3}$$

For consistency with the experimental results, the efficiency is defined as the useful work performed and divided by the product of the volume flow rate, and the drop in static pressure across the turbine:

$$\eta = T\Omega/\dot{Q}(p_1 - p_2) \tag{4}$$

Before discussing the performance predictions, it is necessary to consider the effect on the numerical results of the different meshes used. Figures 3 and 4 show the variations with mesh support of the predictions of pressure drop and torque for the six-blade turbine at $\phi = 0.10$. Here, the reference case is taken from results obtained with a relatively coarse mesh used in an initial study; the results with medium mesh support are taken from the tip clearance study and the finest mesh results are from the solidity study. Because of the 90-deg stagger angle of the Wells turbine, the mesh resolution in the region of the blade leading edge is of more importance to the performance predictions than are the axial and radial mesh distributions. For this reason, the numbers quoted for relative mesh support in Figs. 3 and 4 take account of leading-edge resolution only. They have been calculated from the number of nodes inside a circle of radius $c/4$ centered on the blade leading edge. Pressure drop begins to settle more readily than torque. Interestingly, predictions within 2% of those presented for the medium resolution case were obtained for a mesh identical in every respect, except that the spanwise mesh distribution was symmetrical about midspan, i.e., mesh was concentrated in both the hub and tip regions. This eliminates spanwise mesh distribution as a possible cause of the dips seen in Figs. 3 and 4. The results presented next were obtained with the fine meshes, except where it is stated otherwise.

Measured and predicted values of the pressure drop are compared in Fig. 5. Qualitatively, the predicted variations of pressure drop with flow coefficient are almost linear, as expected. The predicted effect of increasing solidity is to increase the pressure drop at any given value of ϕ, also as expected. Quantitatively, the slopes of the predicted performance curves are higher than the corresponding measurements. The maximum error in Δp^* is about 22%, and the average error is about 15%. In part, the discrepancy may be explained by five factors. First, the experiments were performed at a lower tip Mach number than the calculations. The Prandtl–Glauert correction factor based on tip Mach number is 1.06. Second, the experiments used a NACA 0012 profile, whereas the calculations were performed for NACA 0015 blades. Reference 13 quotes a lower lift curve slope for the thicker profile, giving a thickness correction factor of 0.96. Third, the solidities of the experimental turbines are lower than those of the corresponding analyzed turbines. The difference is about 10%, and because Δp^* rises more rapidly than linearly with σ, a correction factor of 1.15 can be justified from the data. Fourthly, increasing the tip clearance from 1 to 2% may reduce the pressure drop by as much as 6%. Finally, the calculations assume that there are no boundary layers on the hub or casing, so that in these regions the analyzed turbines will be operating at higher angles of incidence than the corresponding experimental turbines. Because it is difficult to put a number on this correction a factor of 1.0 is assumed. Putting these factors together gives an overall correction of 1.10, which is not far off the average difference of 15% that has already been noted. Similar comments can be made about the comparison between measured and predicted torque coefficients, shown in Fig. 6. Both the qualitative and quantitative trends with respect to ϕ and σ are correct. Again, the predicted values are slightly higher than the measured ones, though the error is smaller in this case. This is probably a result of the smaller tip clearance of the experimental turbines, which has a more pronounced effect on torque

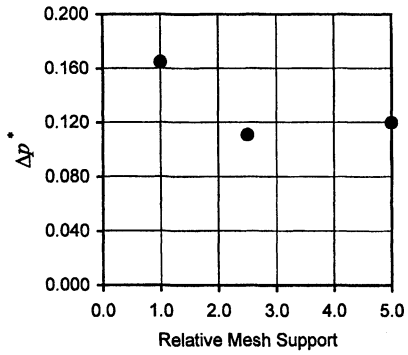

Fig. 3 Variation of Δp^* with relative mesh support.

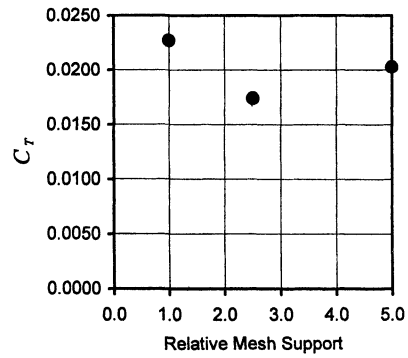

Fig. 4 Variation of C_T with relative mesh support.

than on pressure drop. Increasing the clearance from 1 to 2% can reduce the torque generated by about 10%.

Finally, the comparison between measured and predicted efficiencies is shown in Fig. 7. The calculations have been performed in the range of ϕ, which gives maximum efficiency, and so exhibit neither the rapid rise that occurs at low values of ϕ, nor the sudden drop at the point of stall. The general level of the predicted efficiencies is too high. Combining Eqs. (2–4) gives

$$\eta = (C_T/\Delta p^*)(\Omega R_t^3/\dot{Q}) \tag{5}$$

Because the predicted values of $C_T/\Delta p^*$ are actually too low in each case, the implication is that the predicted values of the volume flow rate ratio $Q_R = \Omega R_t^3/\dot{Q}$ are too high. Assuming that the volume flow rate is used to calculate the mean axial velocity, it can be shown that the ratio of Q_{R1} for a machine with hub-to-tip ratio h_1 to Q_{R2} for a similar machine with hub-to-tip ratio h_2, at the same value of flow coefficient, is given by

$$Q_{R1}/Q_{R2} = (1 - h_2^2)/(1 - h_1^2) \tag{6}$$

The ratio for the analyzed turbines ($h_1 = 0.6$) to the experimental turbines ($h_2 = 0.5$) is therefore 1.17. However, the effect of the larger tip clearance is to reduce efficiency by about 5%. The net increase of 12% explains some of the difference in efficiency between the predictions and measurements.

The predicted effect of tip clearance on turbine performance referred to earlier is illustrated in Figs. 8–10. The calculations were performed at $\phi = 0.10$. As would be expected, increasing tip clearance causes reductions of pressure drop, torque, and efficiency, with the appearance of asymptotic behavior at high clearance. The effect of introducing tip clearance is more pro-

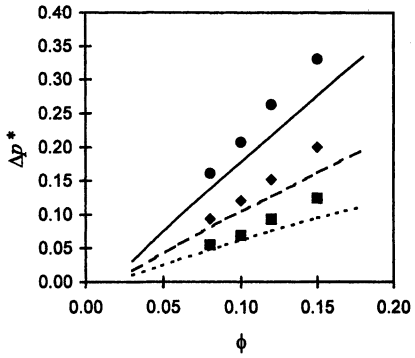

Fig. 5 Pressure drop vs flow coefficient. Measured: —, $N = 4$, $\sigma = 0.29$; – – –, $N = 6$, $\sigma = 0.44$; and ——, $N = 8$, $\sigma = 0.59$. Computed: ■, $N = 4$, $\sigma = 0.32$; ◆, $N = 6$, $\sigma = 0.48$; and ●, $N = 8$, $\sigma = 0.64$.

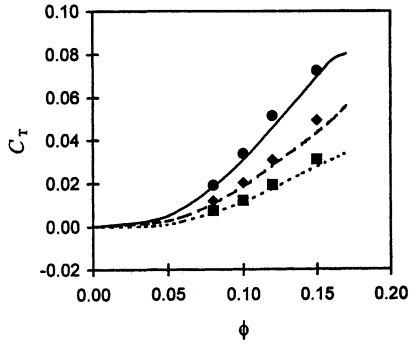

Fig. 6 Torque coefficient vs flow coefficient. Measured: —, $N = 4$, $\sigma = 0.29$; – – –, $N = 6$, $\sigma = 0.44$; and ——, $N = 8$, $\sigma = 0.59$. Computed: ■, $N = 4$, $\sigma = 0.32$; ◆, $N = 6$, $\sigma = 0.48$; and ●, $N = 8$, $\sigma = 0.64$.

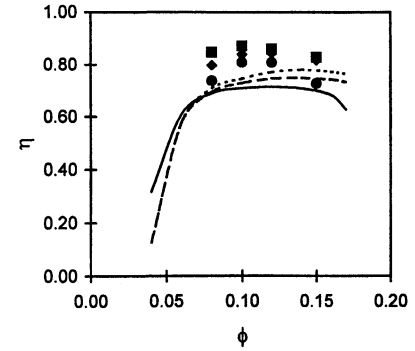

Fig. 7 Efficiency vs flow coefficient. Measured: – – –, $N = 4$, $\sigma = 0.29$; – – –, $N = 6$, $\sigma = 0.44$; and ——, $N = 8$, $\sigma = 0.59$. Computed: ■, $N = 4$, $\sigma = 0.32$; ◆, $N = 6$, $\sigma = 0.48$; and ●, $N = 8$, $\sigma = 0.64$.

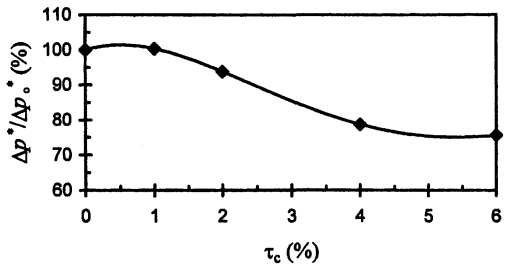

Fig. 8 Pressure drop vs clearance ratio ($\phi = 0.10$).

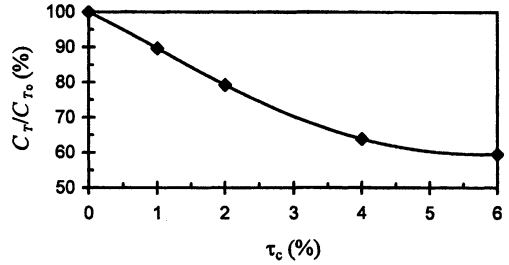

Fig. 9 Variation of torque coefficient with clearance ratio ($\phi = 0.10$).

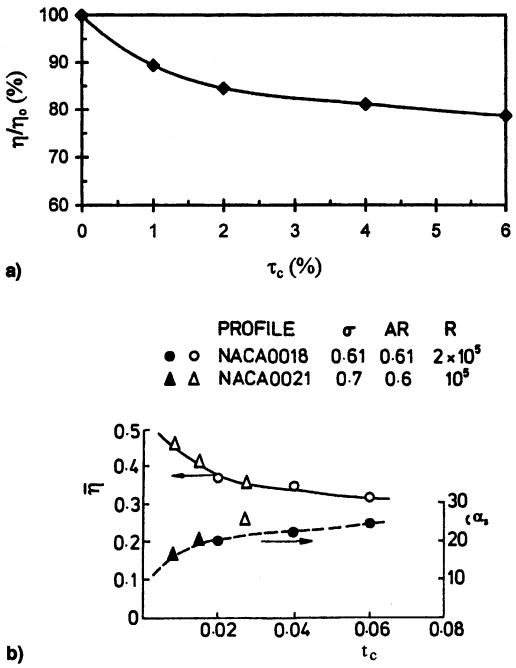

Fig. 10 Calculated and measured variation of efficiency with clearance ratio: a) calculated efficiency vs clearance ratio ($\phi = 0.10$) and b) measured efficiency and stall angle α_s vs clearance.[14]

nounced on torque and efficiency than on pressure drop. This is because the loss of load that the blade sustains when clearance is introduced occurs at maximum radius, giving it a more pronounced effect on torque than on the total load. The predicted effect of clearance on efficiency is confirmed by experimental results[14] shown in Fig. 10b. Although the effect on efficiency of increasing clearance above 2% is small, the reduction in pressure drop that the turbine can sustain is significantly affected, and clearances >2% are not generally recommended.

Turbine Aerodynamics

CFD is able to provide much more information than just the turbine performance. The performance figures are bulk measures of the aerodynamics of the turbine, and it is an advantage of CFD that it allows an investigation of the latter as well as the former. The discussion in this section will be limited to the influence of tip clearance and solidity on the stall limit (and therefore the buffet limit) of the turbine. Although blade stall is very difficult to predict accurately, useful indications of its onset can be gleaned from the calculations.

First consider the effect of tip clearance. Figure 11 shows contours of relative Mach number on planes of constant radius at the turbine hub for the cases with minimum (1%) and maximum (6%) tip clearance at $\phi = 0.10$. The larger suction surface boundary-layer separation clearly occurs in the minimum clearance flow. This is confirmed by Fig. 12, which shows the relative velocity vectors adjacent to the blade suction surface, again for the cases of minimum and maximum tip clearance. In the small clearance flow, there is a region of reversed flow near the blade hub and toward the trailing edge; but there is no evidence of flow reversal in the large clearance vector plot. The difference between the behavior of the small and large clearance flows can be explained by the presence of the tip leakage vortex. Air is pressed through the tip gap by the pressure difference across the blade. As this leakage flow emerges on the suction side, it rolls up to form the tip leakage vortex. This is beneficial to the tip flow because the separation is strong and stable, although it is an important source of loss. The leakage vortex also induces a downwash along the inboard span of the blade, and this reduces the effective incidence of the flow. Hence, the stronger leakage vortex of the larger clearance gap generates a larger reduction of effective incidence than does the smaller clearance flow. And because the blade root is at a lower effective incidence, it is therefore less susceptible to boundary-layer separation. The effect of the leakage vortex is conspicuous by its absence ($\tau_c = 0\%$), e.g., the hub separation is largest.[3]

References 12 and 14 show that increasing solidity increases the value of ϕ at which turbine stall occurs. Predicting the value of ϕ at which stall occurs is very difficult, but some evidence for the influence of solidity can be drawn from the predictions at $\phi = 0.10$. This is illustrated in Figs. 13 and 14.

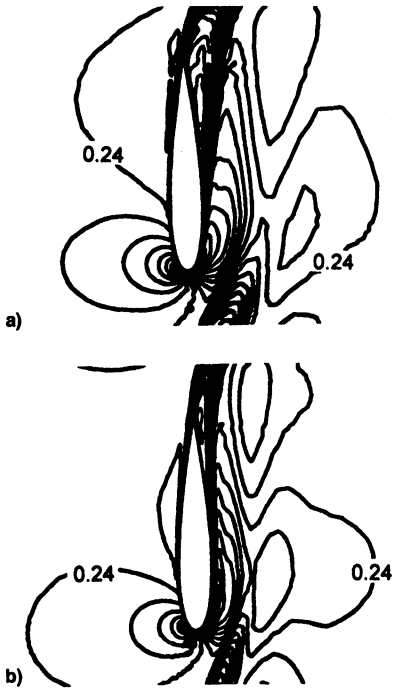

Fig. 11 Relative Mach contours on planes of constant radius at blade root, contour level = 0.02 ($N = 6$, $\phi = 0.1$). τ_c = a) 1% and b) 6%.

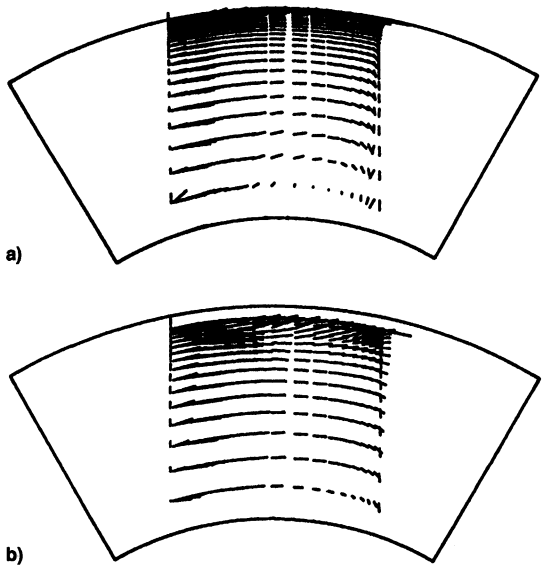

Fig. 12 Relative velocity vectors on the blade suction surface ($N = 6$, $\phi = 0.1$). τ_c = a) 1% and b) 6%.

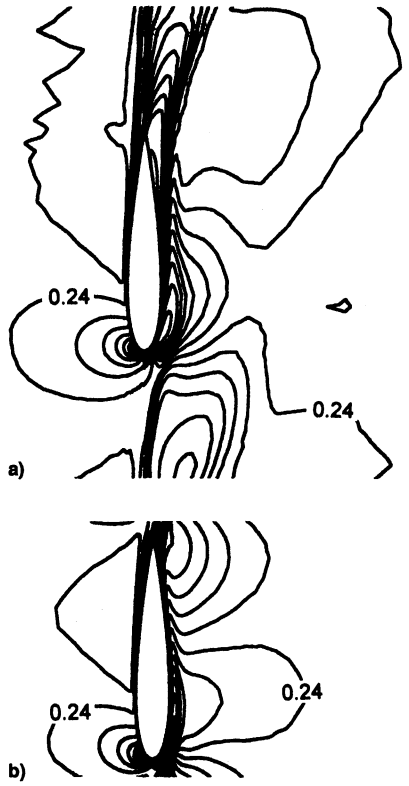

Fig. 13 Relative Mach contours on planes of constant radius at blade root, contour level = 0.02 ($\phi = 0.1$, $\tau_c = 2\%$): a) $N = 4$, $\sigma = 0.32$, and b) $N = 8$, $\sigma = 0.64$.

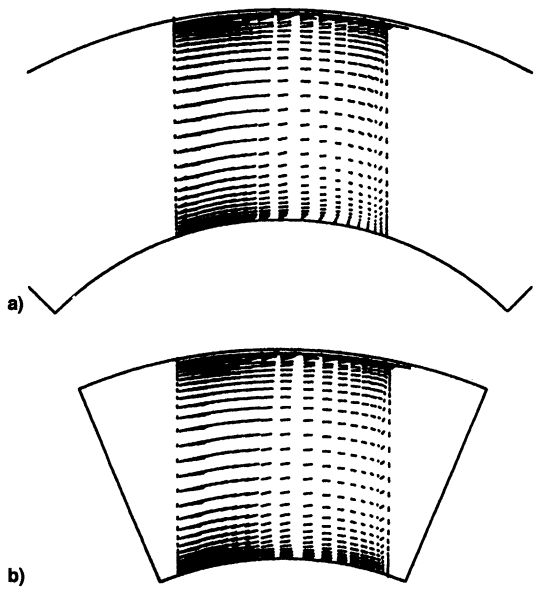

Fig. 14 Relative velocity vectors on the blade suction surface (ϕ = 0.1, τ_c = 2%): a) N = 4, σ = 32, and b) N = 8, σ = 0.64.

Figure 13 shows the contours of relative Mach number at the blade root for the lowest (N = 4, σ = 0.32) and highest (N = 8, σ = 0.64) solidity cases. The higher solidity flow shows much stronger aerodynamic coupling between blade rows. The wake of the upstream blade interacts with the boundary layer developing on the downstream blade, and the boundary layer remains attached over the entire blade chord. In contrast, the lower solidity turbine shows a weaker interaction between upstream and downstream blades, and the boundary layer appears to separate at about 65% chord.

The relative velocity vectors adjacent to the blade suction surface are shown in Fig. 14, for the cases of minimum and maximum solidity. This figure also shows that the lower solidity flow experiences larger hub separation. It is clear that while the flow is fully attached on the suction surface of the higher solidity turbine, there is a small region of reversed flow at the root of the lower solidity case. Increasing turbine solidity influences the flow at the blade root by 1) strengthening the viscous interaction between blades, and 2) redistributing axial flow away from the hub region, thus decreasing the local blade incidence. This delays stall of the hub flow. Conversely, with lower solidity, the hub section would be at higher angle of incidence, and would, therefore, be susceptible to stall at lower values of flow coefficient. Once the hub flow has stalled, the increased blockage causes radial redistribution of the flow, which, in turn, advances stall at higher radii.

Application of CFD to Wells Turbine Calculations

The purpose of presenting the preceding results was to demonstrate that the numerical method is able to 1) predict the turbine performance with reasonable accuracy, and 2) provide some insight to the turbine aerodynamics. Because the numerical method solves discretizations of the correct constitutive equations and is known to be reliable, it is not surprising that the predicted aerodynamics were consistent with what is already known about Wells turbines, and that the performance predictions were accurate. It only remains to discuss the lessons to be learned about the application of CFD to Wells turbine calculations.

First, there is the matter of mesh resolution. Figures 3 and 4 show that fine mesh resolution of the leading edge is essential, if reliable, mesh-independent solutions are to be achieved. This is inevitably expensive, but can be addressed in part by more appropriate meshing strategies than that adopted here. Any meshing strategy, however, must also account for 1) the periodicity of the flow, 2) adequate capture of the blade wakes (particularly as they pass through the periodic boundaries), 3) maintaining good leading-edge resolution for all radii, and 4) meshing of the clearance gap. For a numerical method using unstructured meshes, the Delaunay or advancing front meshing methods would be appropriate.

A second problem for CFD is posed by the order of magnitude difference between the mean axial velocity through the turbine and the blade tangential speed. (This is a consequence of the 90-deg stagger angle of the blades.) Convergence of the solution is slow because the time step of the explicit method is limited by the blade tangential speed plus the acoustic velocity, whereas the convection through the computational domain is limited by the mean axial speed, which is typically less than 5% of the time-step limiting speed. As a consequence, many iterations are required to obtain converged solutions: typically 5000 compared with 1000 for conventional turbine calculations. Possible solutions to this problem are to adopt either a pressure correction method (to avoid the dependence of the time step on the acoustic speed) or an implicit method (to avoid the time-step problem altogether). Shortening of the computational domain would also be beneficial and would be possible if nonreflecting boundary conditions were implemented.

Finally, only simple geometries have been the subject of these studies. The calculations, however, were very time consuming, typically requiring 5 days on a Silicon Graphics Indy workstation, with a 132-MHz IP22 processor and 96 MB of RAM. The exercise was necessary to demonstrate that CFD could reproduce the expected turbine performance and aerodynamics. The method should now be used for the investigation of flows that are not accessible to the simpler predictive tools, e.g., the effect of treatments on the hub, casing, or leading and trailing edges of the turbine blades. It was for these kinds of problems that this particular tool was designed.

Conclusions

The ability of an unstructured mesh CFD method to predict the performance of a monoplane Wells turbine has been tested. It has been shown that good qualitative and predictions of turbine pressure drop and torque have been obtained. The quantitative differences between the predictions and experimental data can be largely explained in terms of the differences between the tip Mach numbers and geometries of the numerical and experimental turbines. Efficiency is overpredicted throughout the range of cases calculated, but some of the difference can be attributed to differences between the hub-to-tip ratios of the numerical and experimental turbines.

Similarly, the predicted turbine aerodynamics are consistent with experimental data. In particular, it has been shown that the predictions indicate that increasing the tip clearance and turbine solidity both have the effect of increasing the resistance of the hub flow to boundary-layer separation: in the former case because of the effect of the tip clearance vortex, and in the latter case because of the strong aerodynamic coupling of blades in the hub region.

Finally, the CFD practitioner should expect Wells turbine calculations to be more computationally expensive than calculations for turbines with lower stagger angles. This is because of two reasons:

1) The accurate prediction of pressure drop and torque depends on sufficiently resolving the leading-edge flow, which requires fine meshes.

2) The order of magnitude difference between the mean axial velocity and the tangential tip speed slows the rate of solution convergence.

Both of these issues must be addressed, and it is recommended that CFD be used only for the study of complex problems inaccessible to simpler predictive methods.

Acknowledgment

The authors express their gratitude to W. N. Dawes for allowing the use of his CFD code, NEWT, in this study.

References

[1]Thorpe, T. W., "A Review of Wave Energy," Department of Trade and Industry, Rept. ETSU-R-72, Dec. 1992.

[2]Whittaker, T. J. T., McIlwain, S. T., and Raghunathan, S., "Islay Shoreline Wave Power Station," European Wave Energy Symposium, Paper G6, Edinburgh, Scotland, UK, Dec. 1990.

[3]Watterson, J. K., and Raghunathan, S., "Computed Effects of Tip Clearance on Wells Turbine Performance," AIAA Paper 97-0994, Jan. 1997.

[4]Watterson, J. K., and Raghunathan, S., "Computed Effects of Solidity on Wells Turbine Performance," *International Journal of the Japanese Society of Mechanical Engineers,* Series B, Vol. 41, No. 1, 1998, pp. 177–183.

[5]Dawes, W. N., "The Practical Application of Solution-Adaption to the Numerical Solution of Complex Turbomachinery Problems," *Progress in Aerospace Sciences*, Vol. 29, 1993, pp. 221–269.

[6]Dawes, W. N., "A Numerical Study of the Interaction of a Transonic Compressor Rotor Overtip Leakage Vortex with the Following Stator Blade Row," American Society of Mechanical Engineers–International Gas Turbine Inst., Paper 94-GT-156, June 1994.

[7]Aubert, S., and Dawes, W. N., "Numerical Analysis of an Axial Flow Fan with Air-Separator Equipment," AIAA Paper 95-2341, Aug. 1995.

[8]Hustad C. W., Savill, A. M., and Dawes, W. N., "A Numerical Investigation of Aerofoil Boundary Layer Manipulator Profile for Cruise Flight Conditions," *Applied Scientific Research,* Vol. 54, 1995, pp. 267–280.

[9]Watterson, J. K., Connell, I. J., Savill, A. M., and Dawes, W. N., "A Solution Adaptive Mesh Procedure for Predicting Confined Explosions," *International Journal for Numerical Methods in Fluids*, Vol. 26, 1998, pp. 235–247.

[10]Lam, C. K. G., and Bremhorst, K. A., "Modified Form of the k-ε Model for Predicting Wall Turbulence," *Journal of Fluids Engineering*, Vol. 103, 1981, pp. 456–460.

[11]Jameson, A., and Baker, T. J., "Improvements to the Aircraft Euler Method," AIAA Paper 87-0452, Jan. 1987.

[12]Gato, L. M. C., and Falcao, A. F. DeO., "Aerodynamics of the Wells Turbine," *International Journal of Mechanical Sciences*, Vol. 30, No. 6, 1988, pp. 383–395.

[13]Abbott, I. A., and Von Doenhoff, A. E., *Theory of Wing Sections*, Dover, New York, 1959.

[14]Raghunathan, S., "The Wells Air Turbine for Energy Conversion," *Progress in Aerospace Sciences*, Vol. 31, 1995, pp. 335–386.